Langmuir

Article

pubs.acs.org/Langmuir

Efficient Control of the Rheological and Surface Properties of Surfactant Solutions Containing C8−C18 Fatty Acids as Cosurfactants

Z. Mitrinova,[†] S. Tcholakova,*[,†] Z. Popova,[†] N. Denkov,[†] Bivash R. Dasgupta,[‡] and K. P. Ananthapadmanabhan[‡]

[†]Department of Chemical Engineering, Faculty of Chemistry and Pharmacy, Sofia University, 1 J. Bourchier Ave., 1164 Sofia, Bulgaria

[‡]Unilever Global Research Center, Trumbull, Connecticut 06611, United States

Supporting Information

ABSTRACT: Systematic experimental study is performed about the effects of chain length (varied between C8 and C18) and concentration of fatty acids (FAc), used as cosurfactants to the mixture of the anionic surfactant SLES and the zwitterionic surfactant CAPB. The following properties are studied: bulk viscosity of the concentrated solutions (10 wt % surfactants), dynamic and equilibrium surface tensions, surface modulus, and foam rheological properties for the diluted foaming solutions (0.5 wt % surfactants). The obtained results show that C8−C10 FAc induce formation of wormlike micelles in the concentrated surfactant solutions, which leads to transformation of these solutions into viscoelastic fluids with very high apparent viscosity. The same FAc shorten the characteristic adsorption time of the diluted solutions by more than 10 times. In contrast, C14−C18 FAc have small effect on the viscosity of the concentrated solutions but increase the surface modulus above 350 mN/m, which leads to higher friction inside sheared foams and to much smaller bubbles in the formed foams. The intermediate chain C12 FAc combines some of the properties seen with C10 FAc and other properties seen with C14 FAc. These results clearly demonstrate how appropriate cosurfactants can be used for efficient control of the rheological properties of concentrated surfactant solutions and of some important foam attributes, such as bubble size and foam rheology.

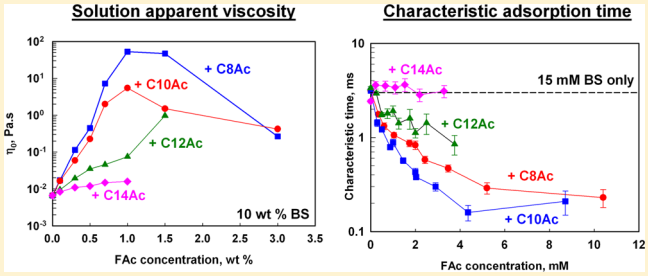

1. INTRODUCTION

Sodium and potassium salts of fatty acids (usually termed as "soaps") are widely studied in literature,[1−22] due to their nontrivial surface properties and numerous applications (e.g., in detergency and floatation). In the course of their studies, researchers have found that the surface properties of soap solutions depend strongly on the fatty acid (FAc) chain length and concentration, pH of the solution, temperature, presence of electrolytes, and so forth.[1−22] Part of this complexity is coming from the relatively high value of the effective pK_a of the FAc (typically between 7 and 11, increasing with FAc chain-length) which leads to multiple equilibria between ionized and neutral acid-soap species.[19] In addition, fatty acids and their salts have limited solubility in water, especially at low pH, which is a major problem in many applications. For example, the soaps stabilize foams at relatively high pH only, around the apparent pK_a of the respective FAc, where the fatty acids are partially soluble in water.[21,22] However, in many cases, higher pH of the solutions is not desired, with the well-known example of skin damage in the case of personal care products.[23,24]

One way to use fatty acids at lower pH is to solubilize them in the micelles of other surfactants.[25−28] In our previous studies,[26,27] we used surfactant mixtures containing an anionic surfactant (SLES) and a zwitterionic surfactant (CAPB) to solubilize myristic and/or lauric acid. In these studies, we used fixed concentrations of all surfactant components, and showed that the solutions containing these long-chain fatty acids (with 14 and 12 carbon atoms) had very high surface modulus, which had an important impact on the foam rheological properties, foam film drainage behavior, and bubble Ostwald ripening in foams, generated from these solutions. The possibility to vary the surface modulus of SLES+CAPB surfactant solutions, by adding lauric and myristic acids, has been utilized already in several studies by other authors to demonstrate the important role of surface modulus on a variety of phenomena, involving bubbles and/or foams.[28−35]

The current study is a direct continuation of our previous work on this topic, with the major aim being now to clarify the effects on the surface properties of the chain length (varied between C8 and C18) and concentration of the fatty acids, when the latter are used as cosurfactants to the SLES+CAPB surfactant mixture. In addition, we study more systematically the relation between the surface properties of the foaming solutions (e.g., kinetics of surfactant adsorption and surface modulus) and the main attributes of the generated foams, such as the mean bubble size in these foams, foam rheological properties, and so forth.

Received: April 7, 2013
Revised: June 6, 2013
Published: June 11, 2013

 © 2013 American Chemical Society dx.doi.org/10.1021/la401291a | *Langmuir* 2013, 29, 8255−8265

To achieve these aims, we performed systematic series of experiments with foaming solutions, containing 15 mM of the basic surfactants (SLES+CAPB) and varied the concentration of fatty acids in the range between 0.02 and 10 mM. The surface properties of these solutions were characterized with respect to the dynamic surface tension, equilibrium surface tension, and dilatational surface modulus. All obtained results are analyzed from the viewpoint of the structure and composition of the formed adsorption layers.

In the course of the current study, we found that the shorter chain fatty acids (C8Ac−C10Ac) are able to induce very strong gelation of the concentrated stock solution of SLES+CAPB (300 mM), while in the absence of fatty acids this solution is Newtonian, with low viscosity. To characterize the rheological properties of these concentrated solutions, we measured their dynamic bulk shear moduli (G' and G'') and their apparent shear viscosity.

The paper is organized as follows: Section 2 describes the materials and methods used. Section 3 describes the experimental results and their discussion. Section 4 summarizes the main results and conclusions.

2. MATERIALS AND METHODS

2.1. Materials. As in our previous studies,[26] the basic surfactant system (denoted as BS) was a mixture of the anionic surfactant sodium dodecyl-oxyethylene ether sulfate (SLES, commercial name STEOL-170, product of Stepan Co.) and the zwitterionic surfactant cocoamidopropyl betaine, CAPB (product of Goldschmith, commercial name Tego Betaine F50). The concentration in the initially prepared concentrated surfactant solution was 10 wt % SLES+CAPB (approximately 300 mM), at fixed weight ratio of 2:1 (corresponding approximately to 200 mM SLES + 100 mM CAPB). The fatty acids were added to the concentrated SLES+CAPB solutions at concentrations that varied from 0.01 to 3 wt %; depending on the FAc molecular mass, this corresponds to the range between 0.1 and 15 mM.

The procedure for preparation of the BS+FAc mixtures was as follows: First, we prepared stock solution of SLES+CAPB with C_{TOT} = 10 wt %. In this concentrated solution, we dissolved the fatty acids, applying heating and mild stirring. Caprylic acid (C8Ac, product of Fluka), decanoic acid (C10Ac, product of Alfa Aesar), and lauric acid (C12Ac, product of Sigma-Aldrich) were dissolved at 40 °C. Myristic acid (C14Ac, product of Sigma-Aldrich) and palmitic acid (C16Ac, product of Riedel-de Haen) were dissolved at 60 °C, while stearic acid (C18Ac, product of Acros organics) was dissolved at 70 °C. These solutions were stored at room temperature at least overnight after their preparation, before conducting any further experiments. The bulk rheological properties of these concentrated solutions were studied as described in section 2.2.

The surface and foam properties were studied as described in sections 2.3−2.8, with solutions obtained after 1:20 dilution of the concentrated stock solution with deionized water.

2.2. Rheological Properties of the Concentrated Surfactant Solutions. The rheological properties of the concentrated solutions were characterized by Gemini rotational rheometer (Malvern Instuments, U.K.), using cone-and-plate geometry, at T = 20 °C. Two different types of experiments were performed. In the first type of experiments, the shear stress as a function of the shear rate was measured. In the second type of experiments, the storage and loss moduli, G' and G'', were measured, as a function of frequency of oscillations, at 2% amplitude of shear deformation.

2.3. Viscosity, Equilibrium, and Dynamic Surface Tension of the Diluted Surfactant Solutions. All diluted solutions were with Newtonian rheological behavior and viscosity close to that of water. Therefore, their viscosity, η, was measured with a thermostatted capillary viscometer, after calibration with pure water. The equilibrium surface tension of the foaming solutions, σ, was measured with the Wilhelmy plate method on tensiometer K100 (Kruss GmbH, Germany). The dynamic surface tension of the solutions was measured with the maximum bubble pressure method on tensiometer BP2 (Kruss GmbH, Germany). All experiments were performed at T = 20 °C.

2.4. Surface Rheological Properties of Diluted Surfactant Solutions. The surface dilatational modulus of the surfactant solutions was measured by the oscillating drop method on a DSA10 instrument, equipped with an ODM/EDM module (Krüss, Germany). The principle of the method is the following: By using a piezo-driven membrane, small oscillations are generated in the volume of a pendant drop (hanging on a needle tip). These oscillations lead to periodical expansions/contractions of the drop surface area: $a(t) = a_0 \sin(\omega t)$, where $a(t) = [A(t) - A_0]/A_0$ is the normalized change of the surface area around the mean area, A_0, while a_0 is the relative amplitude of oscillations and $\nu = 2\pi\omega$ is the frequency of oscillations. Video images of the oscillating drop are recorded and analyzed via the Laplace equation of capillarity to determine the variation of the surface tension, σ, with time. For small deformations, the variation of the surface tension is harmonic:

$$\sigma(t) = G_{SD} a_0 \sin(\omega t) + G_{LD} a_0 \cos(\omega t) \quad (1)$$

where G_{SD} is the surface storage modulus (related to surface elasticity) and G_{LD} is the surface loss modulus (related to surface dilatational viscosity, $\mu_{SD} = G_{LD}/\omega$). The total surface dilatational modulus is

$$G_D = (G_{SD}{}^2 + G_{LD}{}^2)^{1/2} \quad (2)$$

In these experiments, the oscillation frequency was fixed at ν = 0.2 Hz, and the relative area amplitude was varied between 0.2 and 4%. The temperature was kept constant, T = 20 °C, by using a thermostatting chamber TA10 (Krüss, Germany).

2.5. Foam Formation and Mean Bubble Size. The foams were prepared in a planetary mixer (Kenwood Chef Premier KMC 560, 1000 W) which has a homogenization tool with complex geometry, specially designed for efficient air entrapment (see Figure S1 in the Supporting Information). This tool rotates around its own axis like the conventional rotational mixer. In addition, it is attached to a disk, which also rotates around its own axis. As a result, the homogenization tool rotates simultaneously around two axes (see Figure S1). This rotation resembles the movement of the earth around the sun and of the moon around the earth, from where the term "planetary mixer" stems. A volume of 100 mL of the foaming solution was used, and the mixer speed was set at 4, which corresponds to rotational speed of 2 rps and shear rate ≈ 60 s^{-1}, according to the analysis of hydrodynamic conditions made in ref 36. After starting the tool rotation, the volume of trapped air in the foaming solution was measured as a function of time. After a certain period of time, the foam volume remains constant (the air entrapment stops), despite the continuing rotation of the homogenization tool. The rotation continued for at least 5 min after stopping the air entrapment, to be sure that we have reached the final (maximal) foam volume for the given conditions. Immediately after stopping the rotation, we collected foam samples for determination of the mean bubble size, as described in section 2.7. All these experiments were performed at T = 20 °C.

2.6. Foam Generation for Rheological Measurements. To generate foam with fixed air volume fraction, $\Phi \approx 0.9$, we used the following procedure: First, 1 mL of surfactant solution was sucked into a 20 mL syringe, equipped with a stainless steel needle with internal diameter of 2.5 mm (Hamilton, cat. no. 7730-05). Then 9 mL of air was captured in the syringe, forming a coarse foam with large bubbles. These large bubbles were broken into much smaller bubbles, by using a series of ejection/injection cycles of the foam through the needle. In this way, foam containing bubbles of submillimeter diameter was produced.

2.7. Determination of Bubble Size Distribution and Average Bubble Size. Bubble size distribution was determined by using the procedure of Garrett et al.[37,38] The foam is spread in a small Petri dish, and an optical triangular prism is placed on top of the plate, in direct contact with the foam. The foam is illuminated by diffuse white light

through one of the prism sidewalls, whereas the foam observation is made through the other sidewall of the prism via video camera. In the recorded images, one sees as bright spots the wetting films, formed between the bubbles and the prism wall, whereas the Plateau borders around these films are seen as dark interconnected areas. The foam images were processed via a shareware computer program, released by the National Institute of Health (NIH), to determine the bubble size distribution and the mean bubble size. The detailed procedure is described in ref 39.

2.8. Measurement of the Viscous Friction in a Sheared Foam. The rheological properties of the foams were characterized by parallel-plate rheometry on a Gemini rotational rheometer (Malvern Instuments, UK) at T = 20 °C. Sandpaper (P100) was glued on both plates of the rheometer to suppress foam-wall slip. During an experiment, the shear rate, $\dot{\gamma}$, was varied logarithmically from 0.02 to 200 s^{-1} and the shear stress was recorded as a function of shear rate, $\tau = \tau(\dot{\gamma})$. The stress measured in this experiment is due to viscous dissipation in the bulk of the foam. All experiments were performed by using parallel plates with radius of 20 mm, and gap width fixed at 3 mm. Control experiments at smaller gaps (down to 1.5 mm) and stepwise change of the shear rate showed no dependence of the final results on these variations of the conditions.

The obtained results were described very well by Herschel-Bulkley equation, which includes three parameters: yield stress, τ_0; consistency, k; and power-law index, n.

$$\tau = \tau_0 + \tau_V(\dot{\gamma}) = \tau_0 + k\dot{\gamma}^n \quad (3)$$

Here τ is the total shear stress and τ_V is the rate-dependent component which will be termed for brevity "the viscous stress". As discussed in literature,[40−43] it is appropriate to scale the yield stress and the viscous stress by the bubble capillary pressure, $P_C \sim \sigma/R_{32}$, whereas the dimensionless shear rate is represented by the capillary number, Ca:

$$\tilde{\tau}_0 = \frac{\tau_0}{(\sigma/R_{32})}; \quad \tilde{\tau}_V = \frac{\tau_V}{(\sigma/R_{32})}; \quad Ca = \frac{\mu\dot{\gamma}R_{32}}{\sigma} \quad (4)$$

Here $\tilde{\tau}_0$ is dimensionless yield stress, $\tilde{\tau}_V$ is dimensionless viscous stress, and R_{32} is mean volume-surface radius, while σ is surface tension and μ is viscosity of the foaming solution.

3. EXPERIMENTAL RESULTS AND DISCUSSION

The experimental results are described in the following order: The results about the rheological properties of the concentrated solutions are presented in section 3.1. The surface properties of the diluted solutions are described in section 3.2. In section 3.3, we describe the effects of fatty acids on the foam formation, mean bubble size, and foam rheological properties. Section 3.4 is a brief discussion of the relation between the surface properties of the studied solutions and the properties of the foams, generated from these solutions.

3.1. Rheological Properties of the Concentrated Surfactant Solutions. Concentrated solutions, containing 300 mM BS (200 mM SLES + 100 mM CAPB) and fatty acids of different concentrations, were prepared as described in section 2.1. Depending on the fatty acid concentration and chain length, these solutions appeared different in two aspects: (1) turbidity and (2) rheological properties. Because these two characteristics of the concentrated solutions are important to understand the behavior of the diluted foaming solutions, we quantified them using several tests.

The turbidity of the solutions was evaluated by using their visual appearance. We observed a threshold concentration of the fatty acids, above which the turbidity increased very steeply, due to the formation of small droplets (for C8Ac and C10Ac) or crystallites of fatty acids (for the other fatty acids). The threshold concentrations, indicating the solubilization limits of the respective acids in the concentrated SLES+CAPB solutions, were as follows: ≈100 mM C8Ac; ≈85 mM C10Ac; ≈120 mM C12Ac, ≈45 mM C14Ac; ≈25 mM C16Ac; and ≈20 mM C18Ac. From these results, we can calculate the maximum molar fraction of fatty acids, which can be solubilized in the mixed SLES+CAPB micelles:[25]

$$y_{sat} = \frac{C_{FAc,sat}}{C_S + C_{FAc,sat}} \quad (5)$$

where $C_{FAc,sat}$ is the concentration of FAc at the threshold concentration and C_S is the total surfactant concentration (300 mM in our experiments). Taking into account[25] that 100 mM CAPB contains 12.4 mM coco fatty acids (which includes 1.48 mM C8Ac, 1.08 mM C10Ac, 6.65 mM C12Ac, 1.98 mM C14Ac, 0.83 mM C16Ac, and 0.37 mM C18Ac), for the SLES +CAPB mixture we found that y_{sat} ≈ 0.25 for C8Ac, ≈0.22 for C10Ac, ≈0.29 for C12Ac, ≈0.13 for C14Ac, ≈0.077 for C16Ac, and ≈0.063 for C18Ac. These values are in a very good agreement with the results reported by Tzocheva et al.[25] for the solubilization limit of these fatty acids in the micelles of the individual surfactants, SLES and CAPB.

Interestingly, the above results show that C12Ac can be solubilized to the largest extent, as compared to the other fatty acids with shorter and longer chain lengths. These results demonstrate the existence of an optimal chain length, corresponding to a better packing of C12Ac in the micelles of CAPB and SLES.

We observed that the addition of C8Ac or C10Ac to 300 mM BS solution increased significantly the viscosity of these solutions and induced their gelation. To characterize the viscoelastic properties of these concentrated solutions, we measured the solution shear stress, as a function of shear rate. Below certain concentration of FAc, the solution rheological properties were of Newtonian type, and from the slope of the line stress versus rate of strain we determined the viscosity of these solutions. Above a certain FAc concentration, the curve for stress versus rate of strain differed significantly from the linear dependence and acquired the features, characterizing solutions of entangled wormlike micelles. Namely, the shear stress increased linearly with the shear rate, at low shear rates, followed by a wide plateau where the shear stress remained almost constant with the further increase of the shear rate.[44−52]

As an illustration of this behavior, we show in Figure 1 the obtained results for the apparent viscosity, as a function of the shear rate, for BS+C8Ac solutions with different FAc concentrations. One sees that the viscosity is very low at the

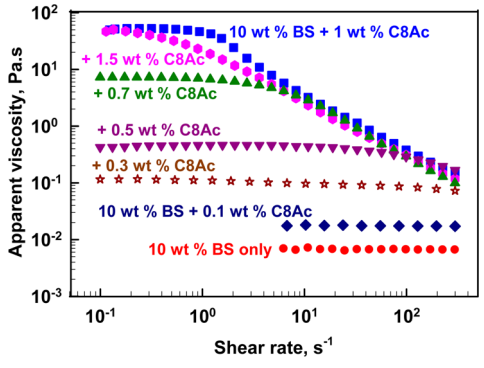

Figure 1. Apparent viscosity as a function of shear rate of micellar solutions of 10 wt % BS only (red circles) and in the presence of C8Ac of various concentrations, as indicated in the figure.

dx.doi.org/10.1021/la401291a | Langmuir 2013, 29, 8255−8265

lowest C8Ac concentration (0.1 wt %) and is practically independent of the shear rate (Newtonian behavior). At higher C8Ac concentrations, the apparent viscosity remains constants at low shear rates and starts to decrease monotonically with the further increase of the shear rate (semi-Newtonian behavior). In the concentration range between 0.7 and 1.5 wt % C8Ac, the samples are gel-like with very high viscoelasticity. It should be mentioned that the solution of 1.5 wt % C8Ac is turbid, but homogeneous; no phase separation was observed in this sample during shelf-storage at room temperature for 1 month. Along with increasing the zero-shear viscosity in the plateau region, the critical shear rate, $\dot{\gamma}_C$, at which the zero-shear viscosity starts to decrease, diminishes with the increase of C8Ac concentration in the micellar solution. The shear thinning above $\dot{\gamma}_C$ is explained in the literature[44−52] by alignment of the wormlike micelles along the flow, when the fluid deformation is faster than the characteristic time for restoring the equilibrium network structure of the micellar solution.[49]

To compare all solutions studied, we determined their zero-shear viscosities and plotted them in Figure 2, as a function of

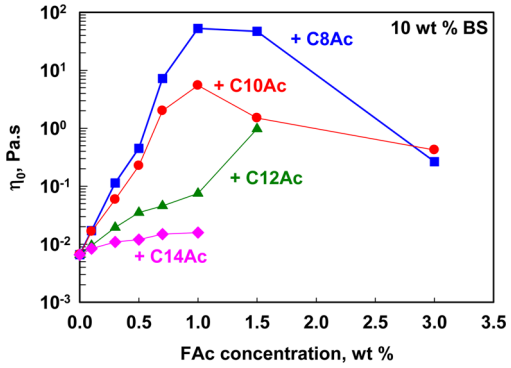

Figure 2. Apparent shear viscosity as a function of fatty acid concentration in 10 wt % BS solution for C8Ac (blue squares), C10Ac (red circles), C12Ac (green triangles), and C14Ac (pink diamonds).

FAc concentration. One should mention that the solutions, containing C12Ac at $C_{FAc} \leq 0.3$ wt % and C14Ac at all studied FAc concentrations, behaved as Newtonian fluids at shear rates above 10 s^{-1} and these values are plotted in Figure 2. We did not perform experiments with solutions, in which phase separation was observed upon shelf storage; therefore, some of the curves in Figure 2 are incomplete.

One sees from the results shown in Figure 2 that η_0 initially increases exponentially with the increase of C8Ac and C10Ac concentrations and passes through a maximum at C_{FAc} = 1 wt %, with maximum values of 55 Pa·s for C8Ac and to 5 Pa·s for C10Ac. These values are 3−4 orders of magnitude higher than the viscosity of the original BS solution without fatty acids (6.6 mPa·s). The highest viscosity for BS+C12Ac solutions (≈1 Pa·s) was measured at C_{FAc} of 1.5 wt %, while the further increase of C12Ac concentration led to formation of precipitate. The addition of C14Ac to BS solution increased the viscosity around 3 times only (16 vs 6.6 mPa·s). Therefore, the fatty acid chain length has a crucial role for the observed effect on the rheological properties of the concentrated BS solutions. The significant decrease of the maximum zero viscosity, while increasing the fatty acid chain length, means that C8 and C10 fatty acids lead to formation of entangled wormlike micelles (see the further explanations below), while the long chain fatty acids probably lead to formation of smaller micelles.

To characterize further the rheological properties of the viscoelastic solutions, we performed oscillatory measurements with BS+C8Ac and BS+C10Ac solutions, at 1 wt % fatty acid. Figure 3A shows the results for G' and G'' as functions of the

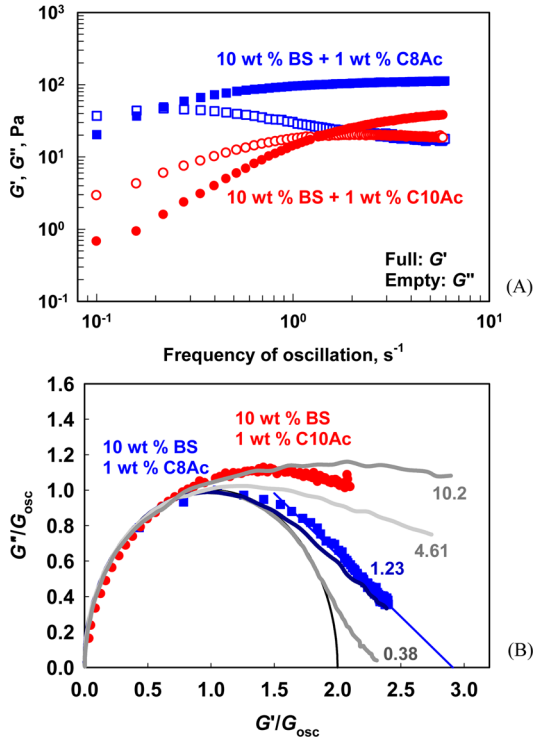

Figure 3. (A) G' (full symbols) and G'' (empty symbols) as a function of oscillation frequency for 10 wt % BS + 1 wt % C8Ac (blue squares) and 10 wt % BS + 1 wt % C10Ac (red circles). (B) Cole−Cole plot for the same systems. The curves represent theoretical calculations from ref 55.

frequency of oscillations, at 2% shear deformation. One sees that the systems behave as liquidlike ($G'' > G'$) at low oscillation frequency. However, at higher oscillation frequency, G' becomes larger than G''. From the crossover of G' and G'', we determined the characteristic frequency, ω_R, which can be used to determine the relaxation time of network restructuring, $t_R = 1/\omega_R$. From the experimental data, we determined $t_R \approx 5$ s for BS+C8Ac and $t_R \approx 0.7$ s for BS+C10Ac solutions.

The viscoelastic behavior of solutions of entangled micelles is described by the Cates model,[53,54] which considers two processes of stress relaxation: "reptation" and "reversible scission" of the micelles. These two processes are associated with two characteristic times: reptation time, t_{rep}, and breaking time, t_{br}. At low frequency of oscillation, these micellar solutions are predicted to obey the Maxwell model, with a single combined relaxation time of $T_R = (t_{rep}t_{br})^{1/2}$. At high frequency of oscillation, the rheological response of the wormlike micelles deviates from the Maxwell model. To check whether our systems have the rheological response of this class of systems, we plotted the experimental data from the oscillatory experiments in a Cole−Cole plot; see Figure 3B. This plot shows that, indeed, the experimental data deviate from the theoretical curve at high oscillation frequencies. Such behavior was observed experimentally before[47] with micellar

dx.doi.org/10.1021/la401291a | Langmuir 2013, 29, 8255−8265

solutions of the cationic surfactant CTAB, in the presence of the electrolyte KBr, and was explained theoretically by the extended model of Turner and Cates.[50] This model allows one to calculate the stress relaxation modulus at different ratios of the breaking and reptation times, $\bar{\zeta} = t_{br}/T_R$. It was shown[50] that, at small $\bar{\zeta}$, the stress relaxation is exponential and the system behaves as a Maxwell fluid, whereas at higher $\bar{\zeta}$ a deviation from the exponential Maxwellian relaxation is observed.[55] By comparing our experimental data in Figure 3B with the theoretical results, presented in ref 52 at different $\bar{\zeta}$, we can estimate that $\bar{\zeta} = t_{br}/T_R \approx 1.23$ for BS+C8Ac and ≈10.2 for BS+C10Ac systems, which explains the observed deviations from the Maxwell behavior of these systems. The value of T_R can be estimated from the ratio of η_0 and G_e. For BS+C8Ac, $T_R \approx 0.5$ s, and for BS+C10Ac $T_R \approx 0.14$ s. Therefore, we can estimate that the breaking time is $t_{br} \approx 0.6$ s and $t_{rep} \approx 0.4$ s for BS+C8Ac micelles, whereas $t_{br} \approx 1.4$ s and $t_{rep} \approx 0.01$ s for BS +C10Ac micelles.

The main conclusions from this series of experiments are as follows: C12Ac has the highest solubility and C18Ac has the lowest solubility in SLES+CAPB micelles, compared to the other fatty acids studied. The shorter chains C8Ac and C10Ac induce strong gelation of 10 wt % SLES+CAPB solution, and increase the apparent viscosity of these solutions by 3−4 orders of magnitude. The rheological behavior of these solutions is typical for solutions containing entangled wormlike micelles, whereas a weaker network is formed when fatty acids with longer chain lengths are used. The zero-shear viscosity for given fatty acid passes through a maximum, when the concentration of fatty acid is increased, and this maximum appears soon before the FAc precipitates out the micelles.

3.2. Surface Properties. In this section, we present experimental results about the equilibrium surface tension (section 3.2.1), dynamic surface tension (section 3.2.2), and surface modulus (section 3.2.3) of the diluted micellar solutions.

We should note that all diluted surfactant solutions (15 mM BS ± FAc) were of Newtonian type, with viscosity very close to that of water, ≈1 mP·s. Also, all clear concentrated solutions remained clear after dilution, while all turbid concentrated solutions gave translucent or opaque diluted solutions.

3.2.1. Equilibrium Surface Tension. The equilibrium surface tension of the diluted solutions was measured by Wilhelmy plate method at $T = 20$ °C. All solutions contained 15 mM BS surfactants (2:1 SLES+CAPB), whereas the concentration of FAc was varied between 0.02 and 10 mM. The obtained results for the equilibrium surface tension, σ_{eq}, are compared in Figure 4. The upper horizontal line represents the surface tension of the original 15 mM BS solution without fatty acids added, $\sigma_{eq} \approx 28.3 \pm 0.4$ mN/m. Note that 15 mM BS is approximately 30 times above the CMC ≈ 0.5 mM of this surfactant mixture.

One sees from Figure 4 that all fatty acids studied are able to decrease σ_{eq} below 28.3 mN/m. The largest decrease is observed when C12Ac, C14Ac or C16Ac is added. These fatty acids are able to decrease σ_{eq} down to 22 ± 0.2 mN/m, which is the typical value for the hydrocarbon−air interface.[55] The concentration required to reach this very low surface tension is ≈1 mM for C14Ac, 1.5 mM for C16Ac, and 7.5 mM for C12Ac. The higher concentration of C12Ac, required to reach $\sigma_{eq} \approx 22$ mN/m, is related to the higher solubility of this fatty acid in the surfactant micelles, as described in section 3.1 above.

C8Ac and C10Ac are also able to decrease significantly the surface tension of BS solution, but it remains higher than that

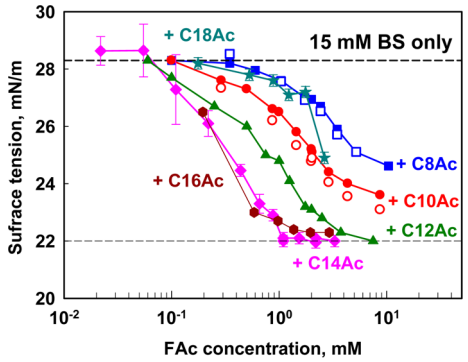

Figure 4. Equilibrium surface tension as a function of fatty acid concentration for fatty acids with different chain lengths, as indicated in the figure. All experiments are performed with 15 mM SLES+CAPB at 2:1 ratio, at $T = 20$ °C.

of solutions containing C12Ac to C16Ac. The minimal surface tensions obtained in 15 mM BS + 10 mM of C10Ac and C8Ac are 23.6 and 24.6 mN/m, respectively. Therefore, the shorter fatty acids lead to higher equilibrium surface tension in the triple solution, which indicates poorer packing inside the equilibrium adsorption layers (note that these fatty acids have lower solubility in the micellar solutions than C12Ac).

Interestingly, we observed that C18Ac is less efficient to decrease σ_{eq}, compared to C12−C16 fatty acids; see Figure 4. In fact, the effect of C18Ac is comparable to that of C8Ac up to 2 mM. However, as shown in section 3.2.2 below, the kinetics of adsorption for C8Ac and C18Ac is very different, which indicates that the observed similar effect on σ_{eq} is a coincidence (compensation of different effects).

In our previous study[56] we explained the surface tension decrease by C14Ac with the formation of mixed adsorption layer of SLES, CAPB, and C14Ac on the solution surface. This explanation is in a good agreement with the results presented in the current study as well. The fact that the largest effect on σ_{eq} is seen with C12−C16Ac can be explained with the formation of mixed adsorption layers, in which these fatty acids have comparable chain length to that of the main surfactants; see Figure S2 for the chemical structure of these surfactants. The fact that C18Ac cannot decrease efficiently the surface tension suggests that these molecules are not incorporated well in the mixed adsorption layer (they are too long). Note that if the adsorption layer was exclusively formed from fatty acids (i.e., composed of molecules with the same chain length), we would expect C18Ac to build a compact homogeneous layer and to have similar effect as C14Ac with σ_{eq} around 22 mN/m.

The main conclusions from these series of experiments are as follows: Mixed adsorption layer of SLES, CAPB, and fatty acid are formed on the surface of BS+FAc solutions. These mixed adsorption layers have much lower surface tension than the surface tension of the individual fatty acids and of the mixed adsorption layer of SLES+CAPB (without fatty acids). The most efficient in decreasing the surface tension are C12−C16 fatty acids, which are able to decrease σ_{eq} down to 22 mN/m (the typical value for the hydrocarbon−water interface).

3.2.2. Dynamic Surface Tension. We measured the dynamic surface tension, $\sigma(t)$, of a series of BS+FAc solutions at different FAc concentrations, as described in section 2.3. The obtained results showed that C16Ac−C18Ac practically do not affect $\sigma(t)$ of the BS solution (data not shown), whereas the shorter fatty acids have a noticeable effect; see Figure 5. The

dx.doi.org/10.1021/la401291a | Langmuir 2013, 29, 8255−8265

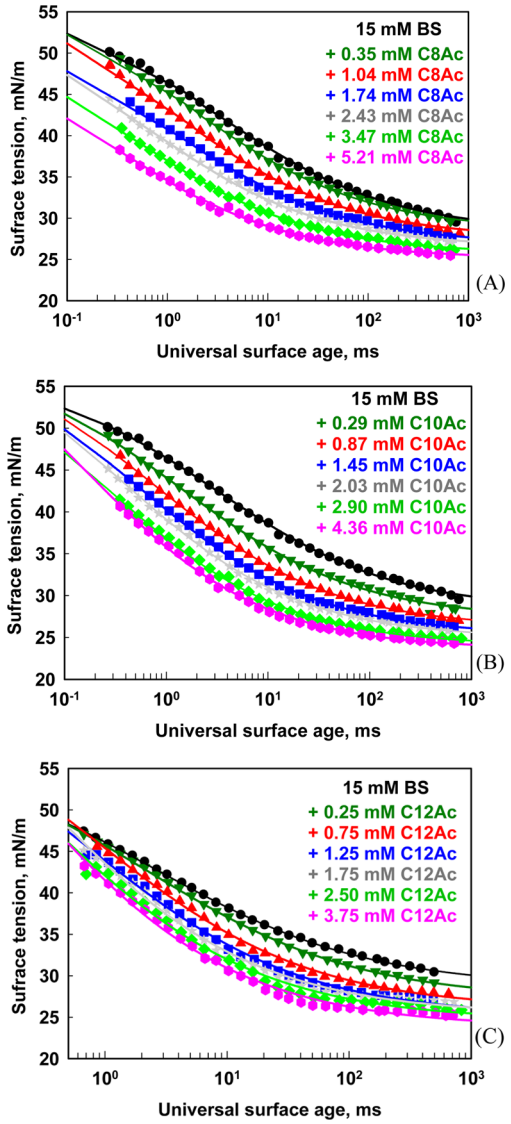

Figure 5. Dynamic surface tension for 15 mM BS solutions in presence of different concentrations of (A) C8Ac, (B) C10Ac, and (C) C12Ac as indicated in the figures. The points are experimental data, whereas the curves are the best fits according to eq 6.

largest effect at shorter times is observed with C8Ac and C10Ac, whereas C12Ac has significant effect at longer times. Therefore, the first important conclusion from these experiments is that the shorter fatty acids (C8Ac−C12Ac) decrease significantly the dynamic surface tension of BS solution, whereas the longer chain fatty acids, C14−C18, which decrease significantly the equilibrium surface tension of BS solution, practically do not affect $\sigma(t)$ at short adsorption times.

To quantify the effect of fatty acids on the adsorption kinetics, we determined the characteristic adsorption time from $\sigma(t)$. For this purpose, the MBPM data were processed in the following way:[57] (1) We plotted the dynamic surface tension as a function of the so-called "universal" surface age, t_u, by applying the correction factor for the used MBPM instrument: $t_u = t_{age}/37$. (2) We fitted the experimental data by the asymptotic equation, proposed in ref 57, for not-too-short adsorption times:

$$\sigma = \sigma_{eq} + \frac{S_\sigma}{a_\sigma} \frac{1}{1 + \sqrt{t_u/a_\sigma^2}} \quad (6)$$

where t_u is the universal surface age, s_σ/a_σ represents the difference between the initial and the equilibrium surface tensions, and a_σ^2 is the characteristic adsorption time.

The curves shown in Figure 5 represent the best fits to the experimental data by eq 6 which contains two adjustable parameters (s_σ and a_σ). It should be mentioned that the fits are particularly good for the solutions containing C8Ac and C10Ac acids; the entire curves (including the long-term asymptotics to σ_{eq}) are described very well by eq 6.

For the solutions containing longer fatty acids, C12Ac−C18Ac, we observed not very large but systematic deviation of the curves from the experimental points at long times. This deviation is most probably due to the formation of surface condensed phase in the mixed adsorption layers, at sufficiently long surface age. On the other hand, at shorter times, the solutions of BS+C14Ac, BS+C16Ac, and BS+C18Ac had dynamic surface tension practically coinciding with that of the BS solution.

The thus determined characteristic adsorption times are compared in Figure 6 for the fatty acids studied. One sees that

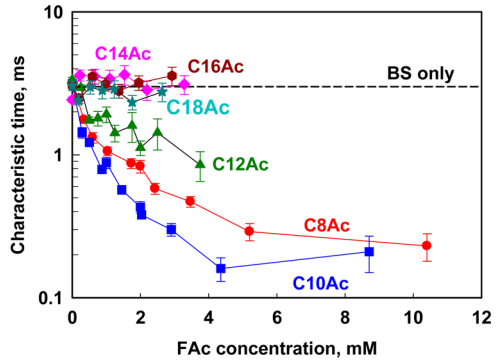

Figure 6. Characteristic adsorption time as determined from the best fits of experimental for $\sigma(t)$ by eq 6 as a function of FAc concentration in the mixture. All solutions contain 15 mM BS.

the characteristic time decreases from 3.3 ms for BS down to 0.3 ms in the presence of 5.2 mM C8Ac in the surfactant mixture. The characteristic time decreases even steeper upon addition of C10Ac; see Figure 6. On the other hand, the long-chain fatty acids (C14−C18) do not affect significantly the characteristic adsorption time of the BS solution, which indicates that the main surfactants adsorb first from these mixtures (without their adsorption kinetics being affected by the FAc) and the long chain fatty acids adsorb afterward. Intermediate behavior is observed for C12Ac.

From this series of experiments, we can conclude that C8−C10Ac shorten significantly the characteristic adsorption time of BS solution, whereas the long-chain fatty acids C14−C16Ac do not affect this time. The intermediate in chain length C12Ac is able to decrease both the characteristic adsorption time and the equilibrium surface tension of BS solution.

3.2.3. Surface Rheological Properties. The surface rheological properties of BS and BS+FAc solutions at C_{FAc} = 1.1 and 3.75 mM for C8Ac−C12Ac were characterized, at 5 s periods of oscillation and surface deformation varied between 0.3 and 2%. The obtained results are shown in Figure 7. One sees that the surface modulus of the C8Ac-containing solution, at 1.1 mM

dx.doi.org/10.1021/la401291a | Langmuir 2013, 29, 8255−8265

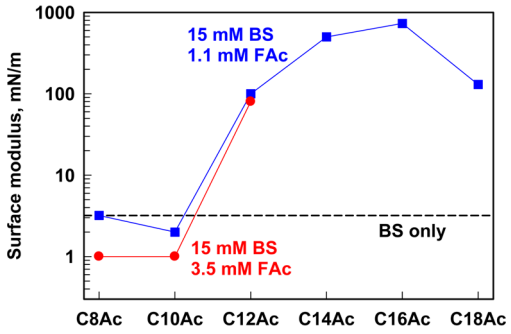

Figure 7. Surface modulus as determined via the ODM module for solutions containing different fatty acids at two different concentrations as indicated in the figure.

FAc, is the same as that for BS solution, whereas the surface modulus decreases from 3 to 1 mN/m at the higher C8Ac concentration (3.75 mM). Similar effect was observed for C10Ac, even at the lower C10Ac concentration studied. Significantly higher surface modulus was determined, $G_D \approx$ 100 mN/m, for the solutions containing the longer fatty acid C12Ac (at both concentrations studied, 1.1 and 3.75 mM). The further increase of the FAc chain length leads to a rapid increase of the surface modulus and the latter becomes higher than 700 mN/m, when C16Ac is added to the BS surfactant mixture. However, the longest fatty acid, C18Ac, leads to lower surface modulus (120 mN/m).

Concluding, the surface modulus of BS+FAc solutions passes through a high maximum around C16Ac, when the fatty acid chain length is varied.

3.3. Foam Properties. In this section, we present experimental results about the mean bubble size (section 3.3.1) and rheological properties of the foams (section 3.3.2), generated from the studied surfactant mixtures.

3.3.1. Bubble Size in the Formed Foams. The experimental results for the foam volume, as a function of the mixing time, for 15 mM BS with and without 1 mM FAc are compared in Figure S3. The curves consist of three well-defined regions: (1) initial fast increase of the foam volume with time; (2) slower further increase of foam volume, and (3) plateau region where the foam volume remains constant, despite the continuing shearing of the system.

The final foam (in the plateau region) was characterized by its volume and by the mean size of the formed bubbles. To quantify the kinetics of foam formation, for each system, we determined the time required for formation of a foam with air volume fraction of 0.89, $t_{\Phi=0.89}$. This particular air volume fraction was chosen because it corresponds to the maximal air volume fraction which can be reached with C14Ac present in the solution; see Figure S3 (the other solutions give higher air volume fraction).

The experimental results for the characteristic foaming time, $t_{\Phi=0.89}$, and the mean volume-surface radius in the plateau region, R_{32}, are compared in Figure 8 for two molar concentrations of the fatty acids (1 mM and 3.5 mM). One sees that C8Ac and C10Ac increase noticeably the rate of foam generation, when compared to the BS solution, especially at the higher concentration studied. The effect of C12Ac on the rate of foam formation depends significantly on its concentration; see Figure 8. At low concentration (1 mM), C12Ac increases slightly the rate of foam generation, whereas at 3.5 mM the same fatty acid decreases significantly the rate of foam

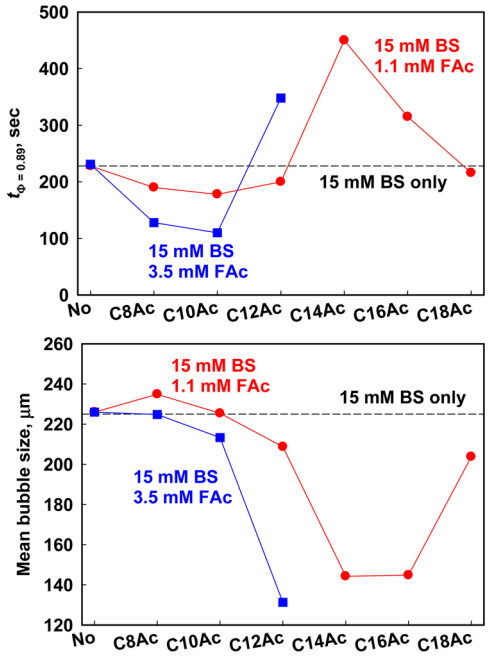

Figure 8. Characteristics of foams formed in the mixer at 2 rps from 150 mL of 15 mM BS in the presence of 1.1 mM (red circles) and 3.5 mM (blue squares) of different fatty acids as indicated in the figure: (top) time required to form foams with air volume fraction of 0.89; (bottom) mean bubble size in the final foam.

generation. This effect is even more pronounced with respect to the final volume of the formed foam. At 1 mM C12Ac, the final foam volume is slightly lower than that for the BS solution while the mean bubble size is similar to that of BS; see Figure 8, bottom. However, at higher C12Ac concentration, the mean bubble size decreases from 220 down to 130 μm, which is accompanied with a significant reduction of the final foam volume, from 2.4 L down to 1.3 L (i.e., almost twice). A similar effect was observed when C14Ac and C16Ac were used as cosurfactants, even at the low concentration of 1 mM.

From these series of experiments, we can conclude that C8Ac and C10Ac lead to faster foam formation, while the mean bubble size and the final foam volume are not affected for foams generated in a planetary mixer, under fixed hydrodynamic conditions. C14Ac and C16Ac fatty acids, which induce phase transition in the adsorption layer, decrease significantly the mean bubble size in the formed foams, but decrease as well the maximum volume of the generated foam. The longest studied fatty acid (C18Ac) has no significant effect on the rate of foam generation, but this fatty acid can decrease to some extent the mean bubble size and the final foam volume. At low concentration (1 mM), C12Ac can increase slightly the rate of foam generation without changing the maximum foam volume and mean bubble size, whereas at higher concentration (3.75 mM) it behaves similarly to C14Ac and C16Ac.

3.3.2. Foam Rheology. The rheological properties of the foams, generated by the procedure described in section 2.8 above, were also measured. All foams in this series of experiments had the same air volume fraction of 0.9. The obtained results for the dimensionless viscous stress, as a function of the capillary number, are compared in Figure 9. As seen from these results, the viscous friction in the foams containing C12Ac−C18Ac is affected strongly by the high surface modulus of the respective foaming solutions. No effect

dx.doi.org/10.1021/la401291a | *Langmuir* 2013, 29, 8255−8265

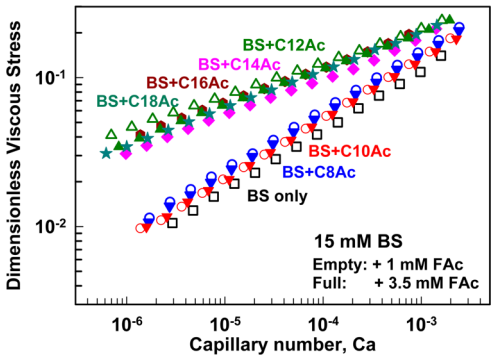

Figure 9. Dimensionless viscous stress as a function of capillary number for foams formed from various BS+FAc mixtures as indicated in the figure. All foams are with air volume fraction of 0.9.

of the fatty acids is seen for BS+C8Ac and BS+C10Ac solutions, which have low surface modulus.

Thus, we reconfirm our previous conclusion[56] that the foams formed from solutions with surface modulus higher than ca. 100 mN/m exhibit much higher dimensionless foam friction, as compared to the solutions with lower surface modulus.

3.4. Discussion of the Relations between the Surface and Foam Properties. Combining all information from the performed experiments, we can draw the following schematic representation of the composition of the adsorption layers at short and long adsorption times (see Figure 10):

(1) At short times, the surfactants present in the solutions containing intermediate chain fatty acids (C8Ac, C10Ac, and C12Ac) adsorb rapidly on the bubble surface and decrease significantly the dynamic surface tension of BS solution. There are two possible mechanisms for this effect of the FAc on dynamic surface tension: (a) The FAc themselves adsorb very rapidly on the surface, thus decreasing faster the surface tension, or (b) the solubilized FAc perturb the micelles of the main surfactants, and as a result, the main surfactant molecules (SLES and CAPB) exchange more rapidly with the surrounding solution and with the surface. At the current moment, we cannot discard completely either of these explanations; however, the accumulated results favor strongly the second explanation (BS micelles perturbed by the FAc). For example, the fact that a very strong effect of C8Ac and C10Ac is observed at rather low concentrations of these acids (0.2 mM FAc in 15 mM BS surfactants) indicates that the observed effect cannot be explained simply by the presence of more molecules (those of the fatty acids) able to adsorb on the surface. In addition, the results with the concentrated BS solutions show that even a very small fraction of C8AC and C10Ac in the mixture (1:50 by weight, which corresponds to molar ratio of 1:25) is sufficient to perturb strongly the micelle structure and the resulting viscosity of the concentrated micellar solutions; see Figure 2.

(2) At longer times, mixed adsorption layer of SLES+CAPB +FAc is formed on the solution surface, which is characterized with lower equilibrium surface tension than that of the BS solution. The long-chain fatty acids C14−C16Ac induce a phase transition in the mixed adsorption layers, with the formation of surface condensed phase, leading to surface with very high surface modulus. The short chain fatty acids are unable to induce surface phase transition at room temperature and, as a consequence, the surface modulus of the respective solutions is very low. For C12Ac and C18Ac, the surface modulus is intermediate, which shows that these fatty acids induce phase transition, but are less efficient in forming well packed adsorption layers.

To understand the observed relations between the surface properties of the studied solutions and their foaming properties, one should consider the two subprocesses of the overall foaming process, namely, the air entrapment, which defines the final volume of the formed foam, and the bubble breakage (subdivision into smaller bubbles), which defines the bubble size distribution in the final foam. At lower surfactant concentrations, two additional processes could become

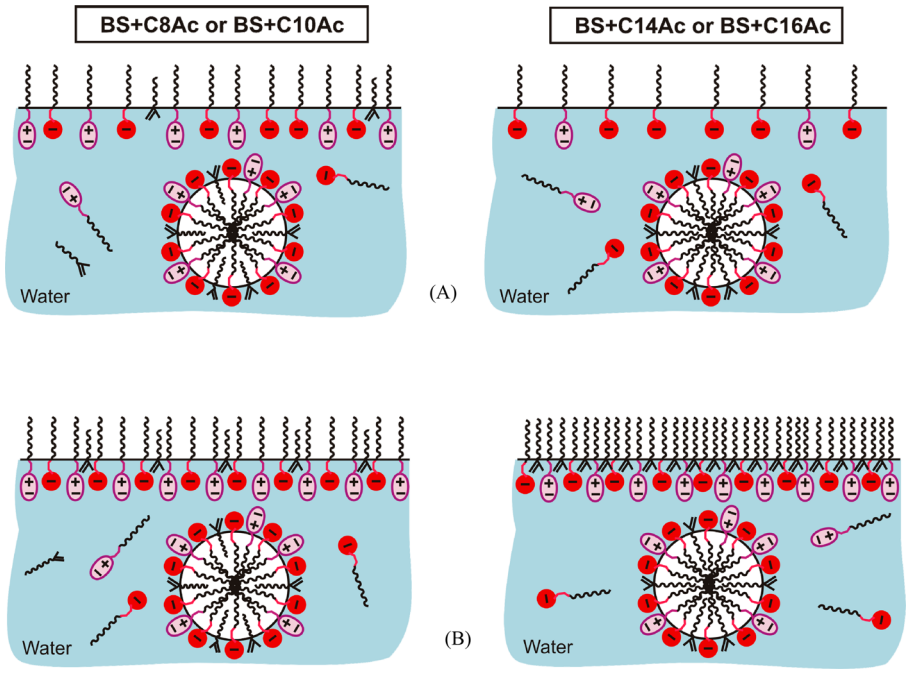

Figure 10. Schematic presentation of the adsorption layers for BS+FAc at (A) short and (B) long time scales.

dx.doi.org/10.1021/la401291a | *Langmuir* 2013, 29, 8255−8265

important: bubble−atmosphere coalescence, which would affect the foam volume, and bubble−bubble coalescence, which would affect the bubble size distribution. However, all foaming experiments in the current study were performed at sufficiently high concentration of the main surfactants SLES+CAPB, so that the coalescence processes are suppressed.

All our results comply with the following coherent picture relating the two main surface properties, dynamic surface tension and surface modulus, with the foaming properties:

As shown in literature[59,60] the volume of the generated foam usually increases with the decrease of the dynamic surface tension of the foaming solution. This relation is typically explained with the easier expansion of the air−water interface upon agitation of the system, which allows bigger bubbles to be trapped in the initial stage of the foaming process. Conceptually, the addition of long-chain fatty acids in the surfactant mixture, which increase the surface modulus of the solution, may reduce the foam volume (as observed in our experiments) by two different mechanisms. First, the expanding surfaces may have higher dynamic surface tension, thus hindering the surface expansion and the related air entrapment process during foaming. However, the measurements of the dynamic surface tension and of the characteristic adsorption time (Figure 6) showed that the long-chain fatty acids do not increase the dynamic surface tension of the foaming solutions, thus ruling out this mechanism.

The second possible mechanism is based on the experimental observation that the foams made from solutions with high surface modulus demonstrate higher viscous friction at otherwise equivalent conditions (e.g., at same bubble volume fraction and shear rate); see Figure 9, for example. Current detailed study of the foaming process in a planetary mixer showed[58] that, at a given shear rate during foaming, the air entrapment stops at a certain effective viscosity of the foam. In the context of our analysis, this result means that the reduced foam volume (viz. the reduced bubble volume fraction) in the presence of C14−C18 FAc compensates for the increased foam viscous friction, caused by the higher surface modulus of the foamed solution.

The observed significant effect of C12−C16Ac on the mean bubble size was investigated and explained in ref 28. It was shown[28] that the higher viscous friction in foams, generated from solutions with high surface modulus, leads to formation of smaller bubbles after foam shearing at given shear rate. The explanation of this effect is rather straightforward: the higher viscous stress in the sheared foams (at given shear rate) leads to more efficient breakage of the bubbles. As shown in ref 28, this relation could be expressed via the critical dimensionless ratio of the foam viscous stress on the bubble capillary pressure, $\tau_{FV}/(\sigma/R_B)$; the experiments showed that the bigger bubbles in sheared foams, for which this ratio is larger than ca. 0.40, would rapidly break into smaller bubbles. Therefore, increasing τ_{FV} (by adding long-chain FAc), we are able to break smaller bubbles at the same shear rate in the planetary mixer.

Thus, we see that the primary effect of the long-chain FAc is to increase the viscous friction in the sheared foams which, in turn, has two important consequences: the air entrapment process is hindered at lower bubble volume fraction (thus reducing the final foam volume), and the initially entrapped large bubbles are broken into smaller bubbles, thus reducing the average bubble size at the end of the foaming process.

4. CONCLUSIONS

Systematic experiments, aimed to clarify the effects of fatty acid chain length and concentration, on the bulk, surface, and foaming properties of SLES+CAPB+FAc solutions were performed. The main results from these experiments could be summarized as follows:

(1) Fatty acid molecules with 8 and 10 carbon atoms induce faster adsorption of the main surfactants (SLES and CAPB) on the bubble surface during foaming. As a consequence, these cosurfactants strongly decrease the dynamic surface tension. The same fatty acids induce formation of wormlike micelles in the concentrated BS solutions, which leads to an increase of the apparent solution viscosity by 3 orders of magnitude (as compared to the concentrated surfactant solution without any fatty acids).

(2) Fatty acid molecules with 14 and 16 carbon atoms, which are comparable to the chain length of the main surfactants (SLES and CAPB), have small effect on the viscosity of the concentrated solutions. However, these fatty acids induce surface phase transition in the adsorption layer, and, as a consequence, these molecules decrease the equilibrium surface tension down to 22 mN/m, increase the surface modulus above 350 mN/m, and increase the friction inside sheared foams. Due to the increased foam friction, the mean bubble size in the formed foams is smaller and the foaminess of the solutions is lower.

(3) Fatty acid with 12 carbon atoms has the highest solubility in BS surfactant micelles. With respect to the other properties, this fatty acid combines some of the properties seen with C10Ac and other properties seen with C14Ac. For example, it decreases the characteristic adsorption time as C10Ac does, while it decreases the equilibrium surface tension down to 22 mN/m, similarly to C14Ac. Solutions containing C12Ac lead to foams containing smaller bubbles, as compared to the foaming solution without fatty acids.

(4) Fatty acid with 18 carbon atoms has the lowest solubility in the mixed SLES+CAPB surfactant micelles. This fatty acid can induce surface phase transition in the adsorption layer and, therefore, increase the surface modulus of the solutions. However, it does not affect the characteristic adsorption time and is not very efficient in decreasing the equilibrium surface tension. As a consequence, this fatty acid has no significant impact on the foaminess of the surfactant solution, but it has significant effect on the mean bubble size and on the foam rheological properties.

The outlined relations between the surface properties (dynamic surface tension and surface modulus) and the foam properties (mean bubble size, viscous friction, and foam volume) seem to be general, as far as the bubble coalescence in the foams is suppressed. Therefore, we expect these relations to be observed in other foaming systems, stabilized by different surfactants.

■ ASSOCIATED CONTENT

Supporting Information

Figure with scheme of (A) Planetary mixer, Kenwood Chef Premier KMC 560, 1000 W. (B) Mixing tool of planetary mixer. (C) Axes of rotation of the mixing tools. Figure with molecular structures of CAPB and SLES. Experimental results for the foam volume, as a function of time, for foams formed in the planetary mixer at 2 rps, from 150 mL of 15 mM BS (black empty circles) and in the presence of 1.1 mM of different fatty

dx.doi.org/10.1021/la401291a | Langmuir 2013, 29, 8255−8265

acids (the other symbols). This material is available free of charge via the Internet at http://pubs.acs.org.

AUTHOR INFORMATION

Corresponding Author

*Phone: (+359-2) 962 5310. Fax: (+359-2) 962 5643. E-mail: SC@LCPE.UNI-SOFIA.BG.

Notes

The authors declare no competing financial interest.

ACKNOWLEDGMENTS

The authors are grateful to Dr. Konstantin Golemanov for the useful discussions and to Miss Diana Cholakova for fitting the experimental data from MBPM and determining the characteristic adsorption times (both from Sofia University). This study is supported by the Unilever R&D Center in Trumbull, CT, USA. The study is under the umbrella of the FP7 European project "Beyond Everest" and the COST action MP1106 "Smart and green interfaces".

REFERENCES

(1) Goddard, E. D.; Kao, O.; Kung, H. C. Monolayer properties of fatty acids: IV. Influence of cation at high pH. *J. Colloid Interface Sci.* **1967**, *24*, 297−309.

(2) Hasmonay, H.; Hochapfel, A.; Peretti, P. Equilibrium position of carboxylic acid molecules in monolayers on aqueous subphases. *J. Colloid Interface Sci.* **1992**, *149*, 247−251.

(3) Daillant, J.; Bosio, L.; Benattar, J. J.; Blot, C. Interaction of cations with a fatty acid monolayer. A grazing incidence X-ray fluorescence and reflectivity study. *Langmuir* **1991**, *7*, 611−614.

(4) Gericke, A.; Hühnerfuss, H. In situ investigation of saturated long-chain fatty acids at the air/water interface by external infrared reflection-absorption spectrometry. *J. Phys. Chem.* **1993**, *97*, 12899−12908.

(5) Gericke, A.; Hühnerfuss, H. The effect of cations on the order of saturated fatty acid monolayers at the air-water interface as determined by infrared reflection-absorption spectrometry. *Thin Solid Films* **1994**, *245*, 74−82.

(6) Gericke, A.; Mendelsohn, R. Partial chain deuteration as an IRRAS probe of conformational order of different regions in hexadecanoic acid monolayers at the air/water interface. *Langmuir* **1996**, *12*, 758−762.

(7) Simon-Kutscher, J.; Gericke, A.; Hühnerfuss, H. Effect of bivalent Ba, Cu, Ni, and Zn cations on the structure of octadecanoic acid monolayers at the air-water interface as determined by external infrared reflection-absorption spectroscopy. *Langmuir* **1996**, *12*, 1027−1034.

(8) Coltharp, K. A.; Franses, E. I. Equilibrium and dynamic surface tension behavior of aqueous soaps: Sodium octanoate and sodium dodecanoate (sodium laurate). *Colloids Surf., A* **1996**, *108*, 225−242.

(9) Chang, C.-H.; Coltharp, K. A.; Park, S. Y.; Franses, E. I. Surface tension measurements with the pulsating bubble method. *Colloids Surf., A* **1996**, *114*, 185−197.

(10) Wen, X.; McGinnis, K. C.; Franses, E. I. Unusually low dynamic surface tensions of aqueous solutions of sodium myristate. *Colloids Surf., A* **1998**, *143*, 371−380.

(11) Wen, X.; Lauterbach, J.; Franses, E. I. Surface densities of adsorbed layers of aqueous sodium myristate inferred from surface tension and infrared reflection absorption spectroscopy. *Langmuir* **2000**, *16*, 6987−6994.

(12) Wen, X.; Franses, E. I. Effect of protonation on the solution and phase behavior of aqueous sodium myristate. *J. Colloid Interface Sci.* **2000**, *231*, 42−51.

(13) Tippmann-Krayer, P.; Mohwald, H. Precise determination of tilt angles by x-ray diffraction and reflection with arachidic acid monolayers. *Langmuir* **1991**, *7*, 2303−2306.

(14) Wantke, K.-D.; Fruhner, H.; Fang, J.; Lunkenheimer, K. Measurements of the Surface Elasticity in Medium Frequency Range Using the Oscillating Bubble Method. *J. Colloid Interface Sci.* **1998**, *208*, 34−48.

(15) Gilman, J. B.; Eliason, T. L.; Fast, A.; Vaida, V. Selectivity and stability of organic films at the air−aqueous interface. *J. Colloid Interface Sci.* **2004**, *280*, 234−243.

(16) Fang, J.; Wantke, K.-D.; Lunkenheimer, K. Rheological Properties of Fatty Acid Solutions at the Air/Water Interface. *J. Colloid Interface Sci.* **1996**, *182*, 31−45.

(17) Albrecht, O.; Matsuda, H.; Eguchi, K.; Nakagiri, T. The dissolution of myristic acid monolayers in water. *Thin Solid Films* **1999**, *338*, 252−264.

(18) Danov, K. D.; Kralchevsky, P. A.; Ananthapadmanabhan, K. P.; Lips, A. Interpretation of surface-tension isotherms of n-alkanoic (fatty) acids by means of the van der Waals model. *J. Colloid Interface Sci.* **2006**, *300*, 809−813.

(19) Kralchevsky, P. A.; Danov, K. D.; Pishmanova, C. I.; Kralchevska, S. D.; Christov, N. C.; Ananthapadmanabhan, K. P.; Lips, A. Effect of the precipitation of neutral-soap, acid-soap, and alkanoic acid crystallites on the bulk pH and surface tension of soap solutions. *Langmuir* **2007**, *23*, 3538−3553.

(20) Petrov, J. G.; Pfohl, T.; Mo1hwald, T. Ellipsometric Chain Length Dependence of Fatty Acid Langmuir Monolayers. A Heads-and-Tails Model. *J. Phys. Chem. B* **1999**, *103*, 3417−3424.

(21) Kanicky, J. R.; Poniatowski, A. F.; Mehta, N. R.; Shah, D. O. Cooperativity among Molecules at Interfaces in Relation to Various Technological Processes: Effect of Chain Length on the pKa of Fatty Acid Salt Solutions. *Langmuir* **2000**, *16*, 172−177.

(22) Kanicky, J. R.; Shah, D. O. Effect of Premicellar Aggregation on the pKa of Fatty Acid Soap Solutions. *Langmuir* **2003**, *19*, 2034−2038.

(23) Shukuwa, T.; Kligman, A. M.; Stoudemayer, T. J. A new model for assessing the damaging effects of soaps and surfactants on human stratum corneum. *Acta Derm.-Venereol.* **1997**, *77*, 29−36.

(24) Ananthapadmanabhan, K. P.; Yang, L.; Vincent, C.; Tsaur, L.; Vetro, K.; Foy, V.; Zhang, S.; Ashkenazi, A.; Pashkovski, E.; Subramanian, V. A novel technology in mild and moisturizing cleansing liquids. *Cosmet. Dermatol.* **2009**, *22*, 307−316.

(25) Tzocheva, S. S.; Kralchevsky, P. A.; Danov, K. D.; Georgieva, G. S.; Post, A. J.; Ananthapadamabhan, K. P. Solubility limits and phase diagrams for fatty acids in anionic (SLES) and zwitterionic (CAPB) micellar surfactant solutions. *J. Colloid Interface Sci.* **2012**, *369*, 274−286.

(26) Golemanov, K.; Denkov, N. D.; Tcholakova, S.; Vethamuthu, M.; Lips, A. Surfactant mixtures for control of bubble surface mobility in foam studies. *Langmuir* **2008**, *24*, 9956−9961.

(27) Denkov, N. D.; Tcholakova, S.; Golemanov, K.; Ananthpadmanabhan, K. P.; Lips, A. The role of surfactant type and bubble surface mobility in foam rheology. *Soft Matter* **2009**, *5*, 3389−3408.

(28) Golemanov, K.; Tcholakova, S.; Denkov, N. D.; Ananthapadmanabhan, K. P.; Lips, A. Breakup of bubbles and drops in steadily sheared foams and concentrated emulsions. *Phys. Rev. E* **2008**, *78*, 051405-1−051405-12.

(29) Tcholakova, S.; Mitrinova, Z.; Golemanov, K.; Denkov, N. D.; Vethamuthu, M.; Ananthapadmanabhan, K. P. Control of Ostwald ripening by using surfactants with high surface modulus. *Langmuir* **2011**, *27*, 14807−14819.

(30) Dorbolo, S.; Terwagne, D.; Delhalle, R.; Dujardin, J.; Huet, N.; Vandewalle, N.; Denkov, N. Antibubble lifetime: Influence of the bulk viscosity and of the surface modulus of the mixture. *Colloids Surf., A* **2010**, *365*, 43−45.

(31) Adami, N.; Dorbolo, S.; Caps, H. Single thermal plume in locally heated vertical soap films. *Phys. Rev. E* **2011**, *84*, 046316-1−046316-8.

(32) Biance, A.-L.; Delbos, A.; Pitois, O. How topological rearrangements and liquid fraction control liquid foam stability. *Phys. Rev. Lett.* **2011**, *106*, 068301−1−068301−4.

(33) Dollet, B. Local description of the two-dimensional flow of foam through a contraction. *J. Rheol.* **2010**, *54*, 741−760.

(34) Emile, J.; Salonen, A.; Dollet, B.; Saint-Jalmes, A. A systematic and quantitative study of the link between foam slipping and interfacial viscoelasticity. *Langmuir* **2009**, *25*, 13412−13418.
(35) Biance, A.-L.; Cohen-Addad, S.; Höhler, R. Topological transition dynamics in a strained bubble cluster. *Soft Matter* **2009**, *5*, 4672−4679.
(36) Chesterton, A. K. S.; Moggridge, G. D.; Sadd, P. A.; Wilson, D. I. Modelling of shear rate distribution in two planetary mixtures for studying development of cake batter structure. *J. Food Eng.* **2011**, *105*, 343−350.
(37) Garrett, P. R.; Hines, J. D.; Joyce, S. C.; Whittal, P. T. Report prepared for Unilever R&D, Port Sunlight, U.K., 1993.
(38) Mukherjee, S.; Wiedersich, H. Morphological and viscoelastic properties of dense foams generated from skin cleansing bars. *Colloids Surf.* **1995**, *95*, 159−172.
(39) Politova, N.; Tcholakova, S.; Golemov, K. G.; Denkov, N. D.; Vethamuthu, M.; Ananthapadmanabhan, K. P. Effect of Cationic Polymers on Foam Rheological Properties. *Langmuir* **2012**, *28*, 1115−1126.
(40) Denkov, N. D.; Subraminian, V.; Gurovich, D.; Lips, A. Wall slip and viscous dissipation in sheared foams: Effect of surface mobility. *Colloids Surf., A* **2005**, *263*, 129−145.
(41) Tcholakova, S.; Denkov, N. D.; Golemanov, K.; Ananthapadmanabhan, K. P.; Lips, A. Theoretical model of viscous friction inside steadily sheared foams and concentrated emulsions. *Phys. Rev. E* **2008**, *78*, 011405-1−011405-18.
(42) Princen, H. M. The structure, mechanics, and rheology of concentrated emulsions and fluid foams. In *Encyclopedia of Emulsion Technology*; Sjöblom, J., Ed.; Marcel Dekker: New York, 2001; Ch. 11, p 243.
(43) Weaire, D. The rheology of foam. *Curr. Opin. Colloid Interface Sci.* **2008**, *13*, 171−176.
(44) Raghavan, S. R.; Fritz, G.; Kaler, E. W. Wormlike micelles formed by synergistic self-assembly in mixtures of anionic and cationic surfactants. *Langmuir* **2002**, *18*, 3797−3803.
(45) Acharya, D. P.; Kunieda, H. Formation of viscoelastic wormlike micellar solutions in mixed nonionic surfactant systems. *J. Phys. Chem. B* **2003**, *107*, 10168−10175.
(46) Aramaki, K.; Hoshida, S.; Arima, S. Formation of wormlike micelles with natural-sourced ingredients (sucrose fatty acid ester and fatty acid) and a viscosity-boosting effect induced by fatty acid soap. *Colloids Surf., A* **2012**, *396*, 278−282.
(47) Kern, F.; Lemarechal, P.; Candau, S. J.; Cates, M. E. Rheological properties of semidilute and concentrated solutions of cetyltrimethylammonium bromide in the presence of potassium bromide. *Langmuir* **1992**, *8*, 437−440.
(48) Khatory, A.; Kern, F.; Lequeux, F.; Appell, J.; Porte, G.; Morie, N.; Ott, A.; Urbach, W. Entangled versus multiconnected network of wormlike micelles. *Langmuir* **1993**, *9*, 933−939.
(49) Shrestha, R. G.; Shrestha, L. K.; Matsunaga, T.; Shibayama, M.; Aramaki, K. Lipophilic tail architecture and molecular structure of neutralizing agent for the controlled rheology of viscoelastic fluid in amino-based anionic surfactant system. *Langmuir* **2011**, *27*, 2229−2236.
(50) Turner, M. S.; Cates, M. E. Linear viscoelasticity of living polymers: A quantitative probe of chemical relaxation times. *Langmuir* **1991**, *7*, 1590−1594.
(51) Granek, R. Dip in $G''(\omega)$ of polymer melts and semidilute solutions. *Langmuir* **1994**, *10*, 1627−1629.
(52) Spenley, N. A.; Cates, M. E.; McLeish, T. C. B. Nonlinear rheology of wormlike micelles. *Phys. Rev. Lett.* **1993**, *71*, 939−942.
(53) Cates, M. E. Reptation of living polymers: Dynamics of entangled polymers in the presence of reversible chain-scission reactions. *Macromolecules* **1987**, *20*, 2289−2296.
(54) Cates, M. E. Nonlinear viscoelasticity of wormlike micelles (and other reversibly breakable polymers). *J. Phys. Chem.* **1990**, *94*, 371−375.
(55) Israelachvili, J. N. *Intermolecular and Surface Forces*, second ed.; Academic Press: New York, 1992.
(56) Mitrinova, Z.; Tcholakova, S.; Golemanov, K.; Denkov, N. D.; Vethamuthu, M.; Ananthapadmanabhan, K. P. Surface and foam properties of SLES + CAPB + fatty acid mixtures: Effect of pH for C12-C16 acids. *Colloid Surf., A* **2012**, DOI: 10.1016/j.colsurfa.2012.12.011.
(57) Christov, N. C.; Danov, K. D.; Kralchevsky, P. A.; Ananthapadmanabhan, K. P.; Lips, A. The Maximum Bubble Pressure Method: Universal Surface Age and Transport Mechanisms in Surfactant Solutions. *Langmuir* **2006**, *22*, 7528−7542.
(58) Tcholakova, S.; Politova, N.; Golemanov, K.; Denkov, N. Mechanism of foam generation in a planetary mixer, **2013**, in preparation.
(59) Patist, A.; Oh, S. G.; Leung, R.; Shah, D. O. Kinetics of micellization: its significance to technological processes. *Colloids Surf., A* **2001**, *176*, 3.
(60) Pandey, S.; Bagwe, R. P.; Shah, D. O. Effect of counterions on surface and foaming properties of dodecyl sulfate. *J. Colloid Interface Sci.* **2003**, *267*, 160.